

# Molecular Dynamics Simulation of Solvent-Polymer Interdiffusion. I. Fickian diffusion

Mesfin Tsige\* and Gary S. Grest†

*Sandia National Laboratories, Albuquerque, NM 87185*

(Dated: October 31, 2018)

## Abstract

The interdiffusion of a solvent into a polymer melt has been studied using large scale molecular dynamics and Monte Carlo simulation techniques. The solvent concentration profile and weight gain by the polymer have been measured as a function of time. The weight gain is found to scale as  $t^{1/2}$ , which is expected for Fickian type of diffusion. The concentration profiles are fit very well assuming Fick's second law with a constant diffusivity. The diffusivity found from fitting Fick's second law is found to be independent of time and equal to the self diffusion constant in the dilute solvent limit. We separately calculated the diffusivity as a function of concentration using the Darken equation and found that the diffusivity is essentially constant for the concentration range relevant for interdiffusion.

---

\* mtsige@sandia.gov

† gsgrest@sandia.gov

## I. INTRODUCTION

The interdiffusion of a solvent into a polymer has been a subject of experimental and theoretical research due to both its scientific and practical importance. There has been a number of studies of penetrant diffusion in homopolymers<sup>1,2,3,4,5,6,7,8,9,10,11,12,13,14,15,16,17,18</sup> but less on interdiffusion of solvent into polymer<sup>19,20,21,22,23</sup> or polymer-polymer interdiffusion.<sup>24,25</sup> Predicting accurately the nature of the interdiffusion of a solvent into a polymer film has turned out to be a challenging problem due to the large number of factors that control the diffusion process, including the molecular weight distribution of the polymer and size of the solvent.<sup>4</sup> Whether the polymer is a melt above its glass transition or an amorphous solid below the glass transition significantly changes the interdiffusion process.

For a polymer melt, if a solvent film is placed in contact with the polymer as shown in Fig. 1, then the diffusion is one-dimensional and can often be described satisfactorily by Fick's second law<sup>26</sup>

$$\frac{\partial c}{\partial t} = \frac{\partial}{\partial z} \left( D(c) \frac{\partial c}{\partial z} \right), \quad (1)$$

where  $c$  is the solvent concentration and  $D(c)$  is the diffusivity. This equation assumes that the volume of the medium is not changed by the interdiffusion of the solvent. In this case the nature of the diffusion is called Fickian or Case I.<sup>27,28</sup> One fingerprint for Fickian diffusion is that the penetration or weight gain by the polymer system increases as  $t^{1/2}$ . In general  $D(c)$  is dependent of concentration  $c$  and Eq. 1 must be solved numerically, except in special cases.<sup>26</sup> If the diffusivity  $D(c) = D_o$  is independent of solvent concentration  $c$  then the solution of Eq. 1 for the concentration of solvent in the medium as a function of time and position is simply

$$c(z, t) = c_0 \left( 1 - \operatorname{erf} \left( z / 2 \sqrt{(D_o t)} \right) \right). \quad (2)$$

Here  $c_0$  is the equilibrium solvent concentration in the polymer usually expressed in units of mass per unit volume and erf is the error function. Even though the solvent in general swells the polymer and  $D(c)$  may not be independent of  $c$ , the simple functional form Eq. (2) is often used to fit experimental data.<sup>29</sup>

For glassy polymers the diffusion process does not always follow the standard Fickian model and is, in general, referred to be anomalous or non-Fickian diffusion phenomena, which is caused by viscoelastic effects in the polymer-solvent system. One type of anomalous behavior, which has been observed experimentally, is called Case II<sup>22,28,30,31,32</sup> in which the polymer

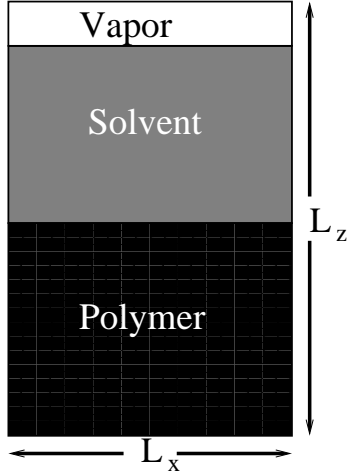


FIG. 1: Schematic representation of the MD simulation box for the interdiffusion study. To allow diffusion in one direction the system is periodic in the  $x$  and  $y$  direction but not in  $z$ . The vapor region is added to keep the pressure constant.

relaxation process is very slow compared to the diffusion and exhibits a sharp concentration front that propagates at constant speed. However, recent careful experiments<sup>19,20,21,22</sup> have shown that a Fickian-like precursor foot precedes the sharp front. To our knowledge no simulations have been done to date on Case II diffusion due to the extensive computational effort required. In this paper we report on our interdiffusion studies of a solvent into a homopolymer above the glass transition temperature, which is expected to exhibit Fickian diffusion behavior. We leave the anomalous interdiffusion into a glassy polymer for a later study.

The transport of penetrant molecules in rubbery polymers has been studied using molecular dynamics (MD) simulation techniques.<sup>2,3,4,5,6,8,9,10,11,12,14,15,18</sup> Most of these studies have focused on the penetrant diffusion of solvent molecules in a polymer to determine the self diffusion constant. The self diffusion constant  $D_s(c)$  of the solvent is easily calculated from the slope of the solvent mean square displacement for long times according to the Einstein relation

$$D_s(c) = \lim_{t \rightarrow \infty} \frac{\langle [\mathbf{r}(t) - \mathbf{r}(0)]^2 \rangle}{6t}. \quad (3)$$

In eqn. 3 the  $\langle \dots \rangle$  denote an ensemble average and is obtained by averaging over all solvents and many initial time origins. In general  $D(c)$  and  $D_s(c)$  are equal only in the dilute solvent

limit,  $c \simeq 0$ .

There have been a number of proposed relations between  $D(c)$  and  $D_s(c)$ , the most common is the Darken equation<sup>33</sup>

$$D(c) = D_c(c) \left( \frac{\partial \ln f}{\partial \ln c} \right)_T \quad (4)$$

where  $D_c(c)$  is called the corrected diffusivity and is related to molecular mobility and  $f$  is the fugacity of the solvent in the polymer. The thermodynamic factor  $\partial \ln f / \partial \ln c$  goes to unity in the dilute limit. Eq. 4 assumes that diffusion is driven by gradients in chemical potential. The corrected diffusivity can be expressed microscopically as<sup>34,35,36</sup>

$$D_c(c) = \frac{1}{3N x_s x_p} \int_0^\infty \langle \mathbf{J}(t) \cdot \mathbf{J}(0) \rangle dt, \quad (5)$$

where  $\mathbf{J}(t)$  is the interdiffusion current,

$$\mathbf{J}(t) = x_p \sum_{i=1}^{N_s} \mathbf{v}_i(t) - x_s \sum_{j=1}^{N_p} \mathbf{v}_j(t). \quad (6)$$

Here  $x_s$  and  $x_p$  are the mole fractions of the solvent and the polymer, respectively and  $N_s$  and  $N_p$  are the number of solvent and polymer monomers. The Einstein form of Eq. 6 is<sup>36</sup>

$$D_c(c) = N x_s x_p \lim_{t \rightarrow \infty} \frac{1}{6t} \langle \{ [\mathbf{r}_{cm,s}(t) - \mathbf{r}_{cm,s}(0)] - [\mathbf{r}_{cm,p}(t) - \mathbf{r}_{cm,p}(0)] \}^2 \rangle \quad (7)$$

where  $\mathbf{r}_{cm,s}(t)$  and  $\mathbf{r}_{cm,p}(t)$  are the center of mass of all solvent monomers and all polymer molecules at time  $t$ , respectively. The Einstein form is preferable to the Green-Kubo form (velocity auto correlation) since it avoids the need to integrate the time correlation functions.

To the best of our knowledge, no MD simulation has been carried out to study the relationship between the interdiffusion of a solvent into a polymer and the diffusivity and self diffusion of solvent in an equilibrated polymer solution. Unlike solvent diffusing in a zeolite<sup>35,37,38</sup> or other microporous media,<sup>39</sup> the polymer swells as the solvent interpenetrates, making it difficult to measure the concentration dependence of the diffusivity  $D(c)$  directly.

Here we are mainly interested in investigating the penetration rates and concentration profiles as a function of time through direct analysis of molecular trajectories for Fickian diffusion in amorphous polymer-solvent systems. We are particularly interested in the relation between the diffusivity  $D(c)$ , the self diffusion constant  $D_s(c)$  and the corrected diffusion constant  $D_c(c)$  for the solvent. Under these circumstances, MD is a useful tool to determine the desired quantities and we have used it for our present study. By combining MD simulation with Monte Carlo<sup>40</sup> methods we can determine all of these quantities.

The paper is organized as follows. In the following section a brief review of the model and the simulation method used is given. The two types of thermostats, Langevin and Dissipative Particle Dynamics (DPD), used in the simulation are also briefly described. In Sec. III the results for the diffusion constants as a function of solvent concentration using the two thermostats are presented. In Sec. IV the interdiffusion results are presented and discussed. Finally, the main results are summarized in Sec. V.

## II. MODEL AND SIMULATION DETAILS

We performed MD simulations of polymer-solvent system using the coarse grained bead-spring model which has been applied successfully to study the effect of entanglement in polymer melts.<sup>41</sup> In this model the polymers are represented by freely jointed bead spring chains of length  $N$  monomers of mass  $m$ . The solvent is modeled as either single monomers of mass  $m$  or dimers of mass  $2m$ . The potential energy associated with interaction between nonbonded monomers of type  $\alpha$  and  $\beta$  is given by the standard Lennard-Jones 6-12 potential

$$U_{LJ}(r) = \begin{cases} 4\epsilon_{\alpha\beta} \left\{ \left( \frac{\sigma_{\alpha\beta}}{r} \right)^{12} - \left( \frac{\sigma_{\alpha\beta}}{r} \right)^6 \right\} + \epsilon_{LJ}, & r \leq r_c \\ 0, & r > r_c \end{cases} \quad (8)$$

where  $r$  is the distance between monomers. Here we take  $\sigma = \sigma_{\alpha\beta}$  and  $r_c = 2.5\sigma$ .  $\epsilon_{\alpha\beta}$  defines the units of energy. In this study we set  $\epsilon = \epsilon_{pp} = \epsilon_{ss}$  where  $p$  stands for a polymer monomer and  $s$  for a solvent monomer and vary the relative interaction  $\epsilon_{sp}$ .

In addition to the Lennard-Jones interaction between bonded monomers we add an anharmonic interaction term known as FENE potential,

$$U(r) = \begin{cases} -0.5R_0^2k \ln [1 - (r/R_0)^2], & r \leq R_0 \\ \infty, & r > R_0 \end{cases} \quad (9)$$

where, as in previous studies<sup>41,42</sup>  $R_0 = 1.5\sigma$  and  $k = 30\epsilon$ .

Our system is also weakly coupled to a heat bath in order to keep it at the desired temperature and as a result each monomer moves according to the following stochastic equation of motion

$$m \frac{d^2 \mathbf{r}_i}{dt^2} = -\nabla \sum_{j \neq i} U(r_{ij}) + \mathbf{F}_i^D + \mathbf{F}_i^R, \quad (10)$$

where  $m$  is the monomer mass,  $U(r_{ij})$  is the sum of the Lennard-Jones and an harmonic spring potential and  $\mathbf{F}_i^D$  and  $\mathbf{F}_i^R$  are the dissipative force and random force, respectively.

These later two terms,  $\mathbf{F}_i^D$  and  $\mathbf{F}_i^R$  together define the type of thermostat used in the simulation. In many simulations of polymer melts, a Langevin thermostat is used in which the particles are coupled weakly to a heat bath. For polymer melts this is a good way to thermostat the system since long range hydrodynamic interactions are screened. However these same interactions are important in the diffusion of small molecules as in the pure solvent. For this reason we have used two types of thermostats: the Langevin thermostat, which by its nature screens the hydrodynamics interactions and the Dissipative Particle Dynamics (DPD) thermostat, which does not.<sup>43,44</sup> Part of the aim of this study is to compare the results for the two thermostats.

### A. Langevin Thermostat

In the Langevin thermostat the dissipative part of the force takes the form of friction that is proportional to the monomer velocity

$$\mathbf{F}_i^D = -m\gamma \frac{d\mathbf{r}_i}{dt}, \quad (11)$$

where  $\gamma$  is the damping constant which is the same for all monomers. The random force is related to the frictional force by the fluctuation/dissipation theorem

$$\langle \mathbf{F}_i^R(t) \cdot \mathbf{F}_j^R(t') \rangle = 6\gamma k_B T m \delta_{ij} \delta(t - t'); \langle \mathbf{F}_i^R(t) \rangle = 0, \quad (12)$$

where  $k_B$  is Boltzmann's constant and  $T$  is the temperature. The damping constant  $\gamma$  controls both the variance of the random force and the magnitude of the frictional force and ensures that the system is kept stable at the desired temperature through out the simulation. However, since the frictional force does not conserve momentum, the hydrodynamic interactions are screened.

### B. Dissipative Particle Dynamics (DPD) Thermostat

DPD has been first introduced<sup>45</sup> and applied to different systems<sup>46,47,48,49,50,51,52</sup> as a mesoscopic simulation technique (not only as a thermostat) to simulate hydrodynamic behavior as well as the rheological properties of complex fluids when thermal fluctuations are important. The fluid is modeled in terms of mesoscopic particles known as dissipative particles that are large quasi-particles, which evolve in the same way as MD particles do, but

with different inter-particle interactions that allow for much longer time steps. The forces between each pair of dissipative particles is made up of a conservative force, a dissipative force and a random force similar to the one given by Eq. 10, but each of which is pairwise additive. These forces in general conserve total momentum and have a spatial range given by the cut-off distance  $r'_c$ . In this case, the dissipative and random forces are the main ingredients for hydrodynamic interaction and are commonly given by,

$$\mathbf{F}_{ij}^D = -m\gamma\omega^D(r_{ij})(\hat{\mathbf{r}}_{ij} \cdot \mathbf{v}_{ij})\hat{\mathbf{r}}_{ij}, \quad \mathbf{F}_{ij}^R = m\sigma\omega^R(r_{ij})\zeta_{ij}\hat{\mathbf{r}}_{ij}, \quad (13)$$

where  $\gamma$  and  $\sigma$  are constants,  $\omega^D(r)$  and  $\omega^R(r)$  are weight functions that vanishes for  $r > r'_c$ ,  $\mathbf{v}_{ij}$  and  $\mathbf{r}_{ij}$  are relative velocity and distance between the pairs, respectively,  $\zeta_{ij}$  is a random noise term with zero mean. The random number can be sampled from either a Gaussian or a uniform distribution, in each case with a variance of unity. Español and Waven<sup>46</sup> have showed that although the weight function can be chosen arbitrarily, it must satisfy the relation  $\omega^D(r) = [\omega^R(r)]^2$ . The friction coefficient  $\gamma$  and the noise amplitude  $\sigma$  are related by the fluctuation/dissipation theorem,  $m\sigma^2 = 2\gamma k_B T$ .

In the present study, however, we used DPD to thermostat the system to take advantage of the fact that it conserves the hydrodynamic interaction between the particles. The function used for  $\omega^D(r)$  and  $\omega^R(r)$  in this study have the following form<sup>51</sup>

$$\omega^D(r) = [\omega^R(r)]^2 = \begin{cases} (1 - r/r'_c)^2, & r < r'_c \\ 0, & r \geq r'_c \end{cases} \quad (14)$$

where we used the same cutoff as for the Lennard-Jones interaction cutoff between monomers,  $r'_c = r_c = 2.5\sigma$ .

All the simulations were run using the massively parallel code LAMMPS.<sup>53</sup> The equations of motion were integrated with a velocity-Verlet algorithm with a time step  $\Delta t = 0.012\tau$  for the interdiffusion study and  $\Delta t = 0.009\tau$  for the bulk equilibrium measurement of the self and corrected diffusion constants, where  $\tau = m(\sigma/\epsilon)^{1/2}$ . The smaller time step was used to assure that the system was stable even for large  $\gamma$  (see Fig. 2). All the simulations were carried out at a temperature of  $T = \epsilon/k_B$  and pressure  $P \simeq 0$ . To determine the fugacity  $f$ , the LADERA grand canonical molecular dynamics (GCMD) code was used.<sup>40</sup> During the course of an equilibrium molecular dynamics simulation at the appropriate solvent concentration, the energy of inserting a solvent particle at random locations was sampled.

The simulated system for the interdiffusion study consists of a rectangular cell, which is periodic in  $x$  and  $y$  direction but not in  $z$  as shown in Fig. 1. This initial configuration was generated in two steps. First, a polymer melt system ( $L_x = L_y = 60\sigma$  and thickness  $L_z \simeq 96\sigma$ ) was equilibrated between two walls at pressure  $P \simeq 0$ . Then the top of the box was extended and the solvent molecules were placed in contact with the polymer melt. Furthermore to keep the pressure of the system constant, a small vapor phase is added between the top wall and the solvent particles. The polymer melts in this study consisted of chains of length  $N = 500$  or 50 monomers. The total number of polymers monomers in all cases was 300,000. The solvent consisted of either 230,000 monomers or 193,000 dimers.

For studying self and corrected diffusion as a function of solvent concentration, the system consists of an equilibrated polymer solvent mixture in a cubic cell, which is periodic in all three directions. The total number of polymer monomers  $N_p = 50,000$  in 100 chains each with 500 monomers. The number of solvent monomers  $N_s$  in the system was varied from 500 monomers (dilute case) to 150,000 monomers. A pure solvent system of 50,000 monomers was also simulated. As the concentration of solvent is varied, the pressure in the system is kept constant by allowing the system relax to the corresponding volume, thus fixing the volume for the measurement of the diffusion constant. Only a few hundred thousand MD timesteps are required to calculate the self diffusion constant  $D_s(c)$  though more than ten times this is required for the corrected diffusion constant  $D_c(c)$ . The fugacity calculation requires approximately a million MC cycles and a few hundred thousand MD timesteps especially at low solvent concentration.

### III. DIFFUSION COEFFICIENTS

#### A. Dependence of self diffusion on the strength of the dissipative force $\gamma$

A set of simulations were performed to determine the dependence of the diffusion on  $\gamma$ . The self diffusion constant,  $D_s(c)$ , of the solvent in the system is calculated using Eq. 3. The results for  $D_s(1)$  are shown in Fig. 2 for the two thermostats.

We find that the values of  $D_s(1)$  from the two thermostats strongly depend on  $\gamma$  and both thermostats show similar dependence. However, for a given value of  $\gamma$ ,  $D_s(1)$  from the two thermostats are not necessarily expected to be equal and the agreement for the two



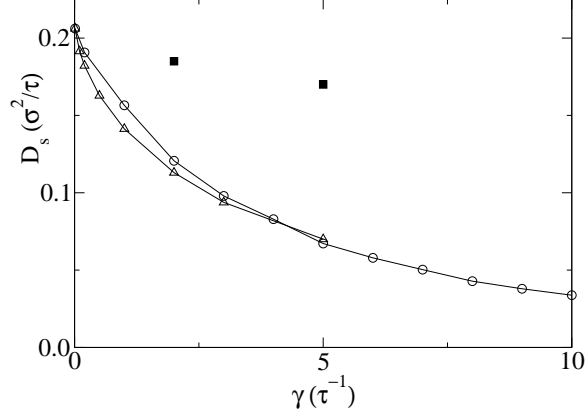


FIG. 2: Dependence of self diffusion constant  $D_s(1)$  for the pure solvent on the damping coefficient  $\gamma$  for the Langevin ( $\Delta$ ) and DPD with  $r'_c = 2.5\sigma$  ( $\circ$ ) and  $r'_c = 2.0\sigma$  ( $\blacksquare$ ) thermostats for  $T = \epsilon/k_B$  and  $P \approx 0$ . The solid lines are a guide to the eye. Error bars are  $\pm 0.002\sigma^2/\tau$ .

thermostats for  $r'_c = 2.5\sigma$  is coincidental. As shown in Fig. 2,  $D_s(1)$  depends not only on  $\gamma$  but also on the cutoff  $r'_c$  in Eq. 14. For small values of  $\gamma$ ,  $D_s(1)$  decreases exponentially, while for large values of  $\gamma$ ,  $D_s(1)$  decreases as  $\gamma^{-1}$  as expected since the random and dissipative forces dominate the interaction between particles and the diffusion becomes Brownian. Note that for large values of  $\gamma$  the Langevin thermostat becomes unstable for the value of timestep used,  $\Delta t = 0.009\tau$ . The strong dependence of  $D_s(1)$  on  $\gamma$  is often ignored specially for DPD particles where large values of  $\gamma$  and large time steps are usually taken. In the rest of our simulation we choose  $\gamma = 0.1\tau^{-1}$  so that the interdiffusion is only weakly affected by the random and dissipative forces.

## B. Concentration dependence of diffusion constants

The self diffusion,  $D_s(c)$ , and corrected diffusion,  $D_c(c)$ , constants are calculated from Eq. 3 and 7, respectively. The calculated values as a function of solvent concentration are shown in Fig. 3. For comparison, the two thermostats with  $\gamma = 0.1\tau^{-1}$  were used to compute the self diffusion. The corrected diffusion constant was determined using the DPD thermostat. The self diffusion values from the two thermostats are the same within the error of the simulation. In general, for low solvent concentration both the self and corrected diffusion constants show weak dependence on concentration. The self diffusion constant then

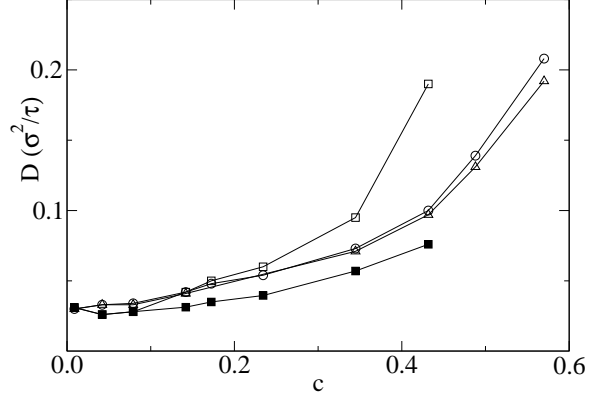


FIG. 3: Dependence of diffusion constants on solvent concentration for  $D_s(c)$  using the Langevin thermostat ( $\Delta$ ) and DPD thermostat ( $o$ ), and  $D_c(c)$  ( $\square$ ) using the DPD thermostat and  $D(c)$  ( $\blacksquare$ ) from Darken equation Eq. 4. For  $c \leq 0.09$ , points for  $D_c(c)$  and  $D(c)$  overlap. The solid lines are a guide to the eye and all results are for polymer chain length  $N = 500$  and  $\epsilon_{12} = \epsilon$ . Error bars are  $\pm 0.002\sigma^2/\tau$ .

increases slowly for intermediate solvent concentration, but a sharp increase is observed for larger concentration.

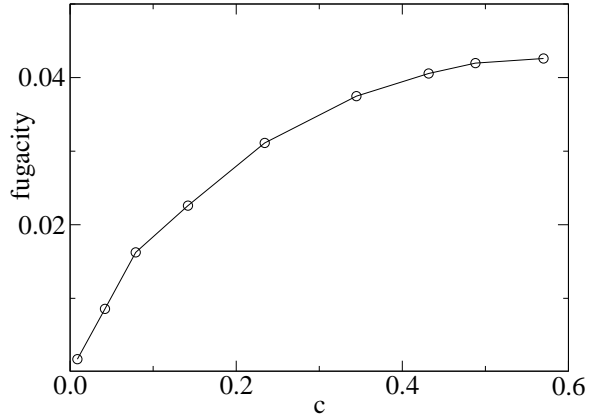


FIG. 4: Fugacity as a function of solvent concentration for monomers in a polymer melt of chain length  $N=500$  and  $\epsilon_{12} = \epsilon$ . Error bars are  $\pm 0.004$ .

To calculate the diffusivity  $D(c)$  from the Darken equation, Eq. 4, the thermodynamic factor  $\partial \ln f / \partial \ln c$  is also required. The fugacity of the solvent was calculated using the GCMD simulation method<sup>40</sup> and is shown in Fig. 4. Numerical differentiation of this data

gives the required thermodynamic factor as a function of solvent concentration. The thermodynamic factor decreases monotonically with concentration opposite to that obtained for solvent in a zeolite or other porous material due to the fact that the solvent swells the polymer, making it easier not harder to insert solvent monomer as the solvent density increases. The diffusivity,  $D(c)$ , calculated from the Darken equation is shown in Fig. 3. Note that  $D(c)$  and  $D_s(c)$  are equal at the dilute limit and show a similar dependence on concentration, though  $D(c)$  increases slower with increasing concentration than  $D_s(c)$ .

#### IV. INTERDIFFUSION

The initial setup for the interdiffusion studies of a solvent into an equilibrated polymer melt is shown in Fig. 1. The density profile, as usually used in experiments, of both polymer,  $\rho_p$  and solvent,  $\rho_s$  as a function of time for the two thermostats is shown in Fig. 5 for a monomer solvent diffusing into a polymer melt of chain length  $N = 500$ . As the solvent diffuses into the polymer, the polymer relaxes and the boundary is smeared out. The density profile at different times for the two thermostats have the same shape differing slightly only in time scale. The rate at which the solvent penetrates into the polymer can be determined either taking a particular value of  $\rho_s$  to define the depth of penetration or by the weight gain by the polymer system as a function of time. The weight gain by the polymer versus  $t^{1/2}$  is shown in Figure 6. Both thermostats give the same result confirming that the penetration increase with  $t^{1/2}$  in agreement with the Fickian diffusion. This can be further justified by plotting the solvent density profiles of Fig. 5 for the DPD thermostat case as a function of  $zt^{-1/2}$  as shown in Fig. 7. The profiles collapse on to a single master curve confirming the Fickian behavior.

As a first approximation we treat  $D(c)$  as a constant  $D_0$  as often done experimentally and fit the solvent concentration profiles of Fig. 7 to the erf function given by Eq. 2. As seen from in Fig. 7(a) (solid line), the erf function fit the concentration profile reasonably well particularly in the low solvent concentration, though overestimates slightly the rate the monomer solvent enters the polymer film near the interface. The diffusivity extracted from the fit in Fig. 7(a) is  $D_0 \simeq 0.033 \pm 0.002 \sigma^2/\tau$  independent of time. This value is within error bars in agreement with  $D(c)$  in the dilute limit,  $D(0) = 0.030 \pm 0.002 \sigma^2/\tau$  from Sec. III.

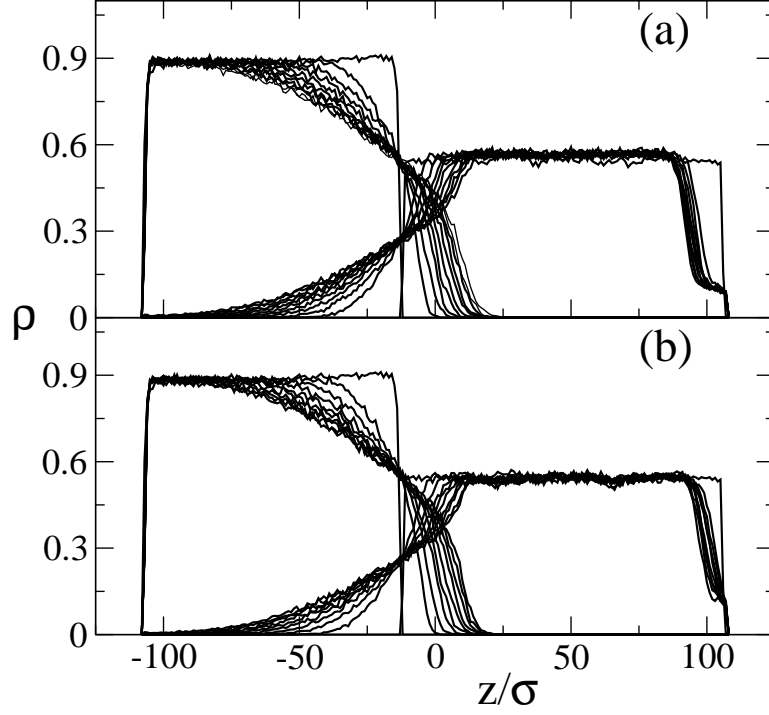


FIG. 5: Solvent  $\rho_s$  and polymer  $\rho_p$  concentration profiles as a function of time starting from  $t = 0$  and plotted every  $2400 \tau$ . The solvent is diffusing into the polymer from the right side and (a) is for the Langevin thermostat and (b) is for the DPD thermostat.

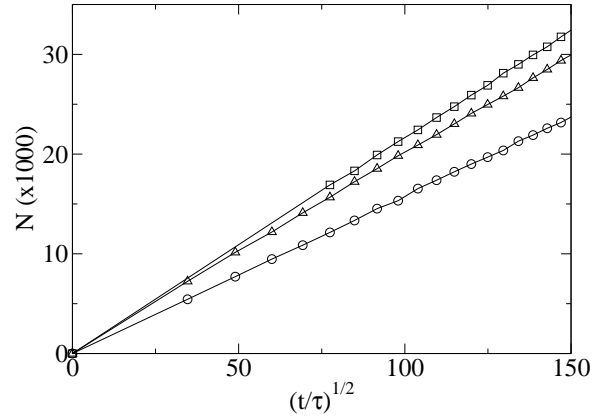


FIG. 6: Weight gain for three solvent-polymer systems, monomer solvent for polymer chain length  $N=500$  ( $\Delta$ ) and  $N=50$  ( $\square$ ) and dimer solvent for chain length  $N=500$  ( $\circ$ ) using DPD thermostat. Similar results for  $N=500$  and monomer solvent were obtained for the Langevin thermostat.

Using the predicted form of  $D(c)$  shown in Fig. 3 from the Darken equation, Eq. 1 can

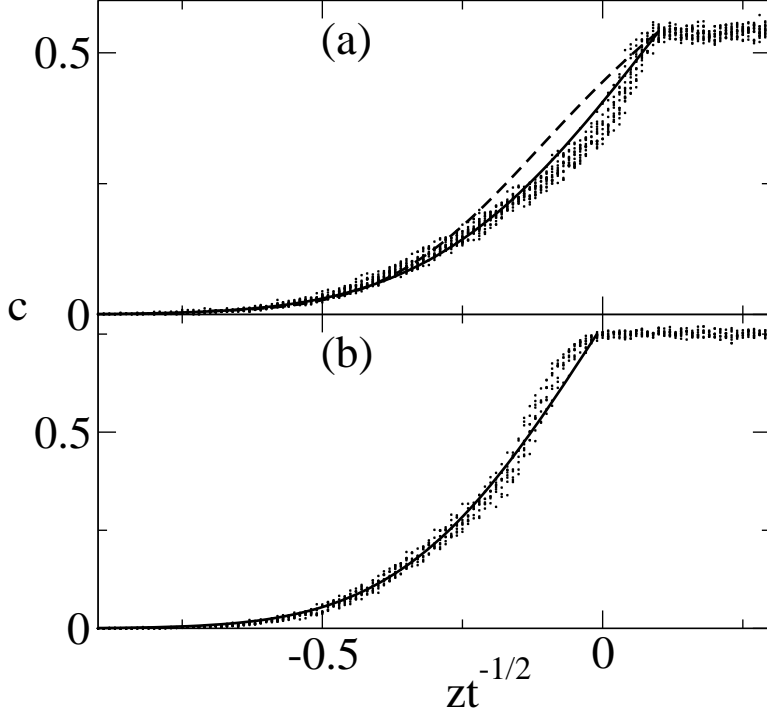


FIG. 7: Solvent concentration profiles are plotted as a function of the scaling variable  $zt^{-1/2}$ , (a) for a monomer solvent that was shown in Fig. 5 and (b) for a dimer solvent. The solid line in both cases is a theoretical fit using Eq. 2 for the profiles. The fit using  $D(c)$  from Fig. 3 is shown as dashed line.

be solved numerically.  $D(c)$  can be fit to  $0.031/(1 - 1.15c)$ . We find the result shown by the dashed line in Fig. 7(a), which fits the simulation result very well at low solvent concentration and overestimates slightly more than constant diffusivity at large concentrations. This deviation at large concentration can be partly attributed to the swelling of the polymer which is neglected in Eq. 1. In Fig. 7(b) we show solvent concentration profiles for the case of dimer solvent and due to the smaller density difference between the solvent and the polymer melt there is less swelling. Since it is difficult to calculate the fugacity for the dimer solvent case we did not calculate the diffusivity as a function of concentration. In this case a constant diffusivity fit (solid line) gives very good agreement with the simulation results even at large concentration. The diffusivity extracted from this fit is  $D_0 = 0.017 \pm 0.001 \sigma^2/\tau$ , which also equaled  $D_s(0)$ . Note that the increase in  $D_s(c)$  from the dilute to the pure solvent limit is about a factor of 6 for the monomer solvent case and a factor of 3.5 for the dimer solvent case. An extrapolation of the fit to the monomer  $D(c)$  gives a factor of 2.9

from the dilute to the pure solvent limit which suggest that for the dimer case  $D(c)$  should increase very slowly with concentration, which further supports the assumption of constant diffusivity.

Our result agrees with the recent hypothesis,<sup>54</sup> based on two-dimensional lattice gas automation simulation, that the nature of the diffusion is not related to the solvent concentration gradient within the system but to the diffusivity gradient ( $dD(c)/dc$ ), and the standard Fickian diffusion only occurs when  $dD(c)/dc \approx 0$ . This justifies the experimental fits to the erf function.

We also explored interdiffusion in a number of different ways, including varying  $\epsilon_{12}$  (polymer-solvent interaction parameter) and polymer chain length. First consider the effect of varying  $\epsilon_{12}$ . For  $\epsilon_{12} = 0.8\epsilon$  the solvent did not diffuse into the polymer melt for the time scale of our simulation. In this case the solvent can be considered to be a poor solvent. On the other hand, for  $\epsilon_{12} = 1.2\epsilon$  little change from the previous Fickian diffusion behavior was observed. For this case the diffusion constant extracted from the error function fit is slightly larger,  $D_0 = 0.037 \pm 0.003 \sigma^2/\tau$ , than for  $\epsilon_{12} = 1.0$ .

To study the effect of the chain length of the polymer we decreased the chain length from  $N = 500$  to  $50$ . As seen from Fig. 6 the diffusion process did not change as expected. The diffusion constant  $D_0$  for a monomer solvent extracted from the error function fit for  $N = 50$  is  $D_0 = 0.035 \pm 0.002 \sigma^2/\tau$  compared to  $D_s(0) = 0.032 \pm 0.002 \sigma^2/\tau$ .

## V. SUMMARY

In this work large scale molecular dynamics and grand canonical Monte Carlo simulation techniques were used to study the interdiffusion of a solvent into a polymer melt. The self and corrected diffusion constants as a function of solvent concentration were determined separately and compared to those obtained from the interdiffusion studies using the Darken equation. For low and intermediate solvent concentration, both  $D_s(c)$  and  $D_c(c)$  increased slowly with solvent concentration and were equal within the error of the simulation. For larger concentrations both diffusion constants increased rapidly with the corrected diffusion constant increasing significantly faster than the self diffusion constant. Because the solvent swells the polymer, the thermodynamic factor  $\partial \ln f / \partial \ln c$  decreased with increased solvent concentration resulting in a diffusivity  $D(c)$  which is essentially constant for low and inter-

mediate concentration and increased less rapidly at high concentration than both  $D_c(c)$  and  $D_s(c)$ . The observed dependence of  $D(c)$  with concentration is opposite to that of a zeolite where  $D(c)$  increases more rapidly with concentration than  $D_c(c)$ .

Fickian diffusion behavior was observed for solvent absorption into polymer melt for all cases studied. This was verified by the  $t^{1/2}$  dependence of the weight gain by the polymer system and thus the diffusion process can be considered to be Fickian. The concentration profile of the solvent fit an error function derived from Fick's second law for constant diffusivity. The diffusivity found from this fit was found to be independent of time and is equal to the self diffusion constant  $D_s(0)$  at the dilute limit. Even though  $D(c)$  is not constant over the entire range of concentration, since it varied little in the low concentration region relevant for interdiffusion, assuming  $D(c)$  constant is a very good approximation.

We also studied the dependence of the interdiffusion on the polymer-solvent interaction strength, the chain length of the polymer and the chain length of the solvent. When the interaction parameter was slightly lowered from the neutral case the solvent did not diffuse into the polymer on the time scale of our simulation. On the other hand, increasing the polymer-solvent interaction parameter by the same amount did not considerably affect the diffusion process. The diffusion process was not also affected by a change in the chain length of the polymer.

Future work will study the crossover from Fickian to non-Fickian diffusion as the state of the polymer changes from a melt to a glass.

## VI. ACKNOWLEDGMENTS

We are thankful to A. P. Thompson for providing the GCMD code and for helpful discussions. Sandia is a multiprogram laboratory operated by Sandia Corporation, a Lockheed Martin company, for the United States Department of Energy's National Nuclear Security Administration under Contract No. DE-AC04-94AL85000.

---

<sup>1</sup> J. S. Vrentas, J. L. Duda, and W. J. Huang, *Macromolecules* **19**, 1718 (1986).

<sup>2</sup> J. Sonnenburg, J. Gao, and J. H. Weiner, *Macromolecules* **23**, 4653 (1990).

<sup>3</sup> H. Takeuchi, R.-J. Roe, and J. E. Mark, *J. Chem. Phys.* **93**, 9042 (1990).

- <sup>4</sup> P. V. K. Pant and R. H. Boyd, *Macromolecules* **25**, 494 (1992).
- <sup>5</sup> F. Müller-Plathe, S. C. Rogers, and W. F. van Gunsteren, *Macromolecules* **25**, 6722 (1992).
- <sup>6</sup> R. M. Sok, H. J. C. Berendsen, and W. F. van Gunsteren, *J. Chem. Phys.* **96**, 4699 (1992).
- <sup>7</sup> A. A. Gusev, S. Arizzi, U. W. Suter, and D. J. Moll, *J. Chem. Phys.* **99**, 2221 (1993).
- <sup>8</sup> Y. Tamai, H. Tanaka, and K. Nakanishi, *Macromolecules* **27**, 4498 (1994).
- <sup>9</sup> R. H. Gee and R. H. Boyd, *Polymer* **36**, 1435 (1995).
- <sup>10</sup> D. Hofman, J. Ulbrich, L. Fritz, and D. Paul, *Polymer* **37**, 4773 (1996).
- <sup>11</sup> T. Li, D. O. Kildsig, and K. Park, *J. Controlled Release* **48**, 57 (1997).
- <sup>12</sup> F. Müller-Plathe, *J. Chem. Phys.* **108**, 8252 (1998).
- <sup>13</sup> M. C. Griffiths, J. Strauch, M. J. Monteiro, and R. G. Gilbert, *Macromolecules* **31**, 7835 (1998).
- <sup>14</sup> O. Hahn, D. A. Mooney, F. Müller-Plathe, and K. Kremer, *J. Chem. Phys.* **111**, 6061 (1999).
- <sup>15</sup> N. F. A. van der Vegt, *Macromolecules* **33**, 3153 (2000).
- <sup>16</sup> M. L. Greenfield and D. N. Theodorou, *Macrol.* **34**, 8541 (2001).
- <sup>17</sup> E. Tocci, D. Hofmann, D. Paul, N. Russo, and E. Drioli, *Polymer* **42**, 521 (2001).
- <sup>18</sup> S. Y. Lim, T. T. Tsotsis, and M. Sahimi, *J. Chem. Phys.* **119**, 496 (2003).
- <sup>19</sup> C. J. Durning, M. M. Hassan, H. M. Tong, and K. W. Lee, *Macromolecules* **28**, 4234 (1995).
- <sup>20</sup> M. M. Hassan and C. J. Durning, *J. Polym. Sci.* **37**, 3159 (1999).
- <sup>21</sup> M. Sanopoulous and F. Stamatialis, *Polymer* **42**, 1429 (2001).
- <sup>22</sup> D. F. Stamatialis, M. Sanopoulous, and J. H. Petropoulos, *Macromolecules* **35**, 1021 (2002).
- <sup>23</sup> M. Tsigis and P. L. Taylor, in preparation (2003).
- <sup>24</sup> W. Jilge, I. Carmesin, K. Kremer, and K. Binder, *Macromolecules* **23**, 5001 (1990).
- <sup>25</sup> H. P. Deutsch and K. Binder, *J. Chem. Phys.* **94**, 2294 (1991).
- <sup>26</sup> J. Crank, *The Mathematics of Diffusion* (Oxford University Press, Oxford, 1975).
- <sup>27</sup> N. J. M. Kuipers and A. A. C. M. Beenackers, *Chem. Eng. Science* **48**, 2957 (1993).
- <sup>28</sup> N. L. Thomas and A. H. Windle, *Polymer* **22**, 627 (1981).
- <sup>29</sup> I. Quijada-Garrido, M. F. de Velasco-Ruiz, and J. M. Barrales-Rienda, *Macromol. Chem. Phys.* **201**, 375 (2000).
- <sup>30</sup> N. L. Thomas and A. H. Windle, *Polymer* **21**, 613 (1980).
- <sup>31</sup> N. L. Thomas and A. H. Windle, *Polymer* **23**, 529 (1982).
- <sup>32</sup> C.-Y. Hui and K.-C. Wu, *J. Appl. Phys.* **61**, 5129 (1987).
- <sup>33</sup> L. S. Darken, *Trans. AIME* **175**, 184 (1948).



- <sup>34</sup> R. Sharma and K. Tankeshwar, J. Chem. Phys. **108**, 2601 (1998).
- <sup>35</sup> E. J. Maginn, A. T. Bell, and D. N. Theodorou, J. Phys. Chem. **97**, 4173 (1993).
- <sup>36</sup> D. N. Theodorou, *Diffusion in Polymers* (Marcel Dekker Inc., New York, 1996).
- <sup>37</sup> A. I. Skoulidis and D. S. Sholl, J. Phys. Chem. B **105**, 3151 (2001).
- <sup>38</sup> M. Chandross, E. B. W. III, G. S. Grest, M. G. Martin, A. P. Thompson, and M. W. Roth, J. Phy. Chem. B **105**, 5700 (2001).
- <sup>39</sup> J. M. D. MacElroy and K. Raghavan, J. Chem. Phys. **93**, 2068 (1990).
- <sup>40</sup> A. P. Thompson and G. S. Heffelfinger, J. Chem. Phys. **110**, 10693 (1999).
- <sup>41</sup> K. Kremer and G. S. Grest, J. Chem. Phys. **92**, 5057 (1990).
- <sup>42</sup> G. S. Grest and K. Kremer, Phys. Rev. A **33**, 3628 (1986).
- <sup>43</sup> B. Dünweg, to be published (2003).
- <sup>44</sup> T. Soddemann, B. Dünweg, and K. Kremer, Phys. Rev. E **to be published** (2003).
- <sup>45</sup> P. J. Hoogerbrugge and J. M. V. A. Koleman, Europhys. Lett. **19**, 155 (1992).
- <sup>46</sup> P. Espanol and P. Warren, Europhys. Lett. **30**, 191 (1995).
- <sup>47</sup> R. D. Groot and P. B. Warren, J. Chem. Phys. **107**, 4423 (1997).
- <sup>48</sup> J. B. Gibson, K. Chen, and S. Chynoweth, J. Colloid and Int. Sci. **206**, 464 (1998).
- <sup>49</sup> J. B. Gibson, K. Zhang, K. Chen, S. Chynoweth, and C. W. Manke, Molecular Simulations **23**, 1 (1999).
- <sup>50</sup> P. Malfreyt and D. J. Tildesley, Langmuir **16**, 4732 (2000).
- <sup>51</sup> J. A. Elliott and A. H. Windle, J. Chem. Phys. **113**, 10367 (2000).
- <sup>52</sup> M. Ripoll, M. H. Ernst, and P. Espanol, J. Chem. Phys. **115**, 7271 (2001).
- <sup>53</sup> S. J. Plimpton, J. Comput. Phys. **117**, 1 (1995).
- <sup>54</sup> M. Küntz and P. Lavallée, J. Phys. D: Appl. Phys. **36**, 1135 (2003).